ARTICLE

doi:10.1038/nature10497

# Diffraction-unlimited all-optical imaging and writing with a photochromic GFP

Tim Grotjohann[1]*, Ilaria Testa[1]*, Marcel Leutenegger[1]*, Hannes Bock[1], Nicolai T. Urban[1], Flavie Lavoie-Cardinal[1], Katrin I. Willig[1], Christian Eggeling[1], Stefan Jakobs[1,2] & Stefan W. Hell[1]

**Lens-based optical microscopy failed to discern fluorescent features closer than 200 nm for decades, but the recent breaking of the diffraction resolution barrier by sequentially switching the fluorescence capability of adjacent features on and off is making nanoscale imaging routine. Reported fluorescence nanoscopy variants switch these features either with intense beams at defined positions or randomly, molecule by molecule. Here we demonstrate an optical nanoscopy that records raw data images from living cells and tissues with low levels of light. This advance has been facilitated by the generation of reversibly switchable enhanced green fluorescent protein (rsEGFP), a fluorescent protein that can be reversibly photoswitched more than a thousand times. Distributions of functional rsEGFP-fusion proteins in living bacteria and mammalian cells are imaged at <40-nanometre resolution. Dendritic spines in living brain slices are super-resolved with about a million times lower light intensities than before. The reversible switching also enables all-optical writing of features with subdiffraction size and spacings, which can be used for data storage.**

In a fluorescence microscope, diffraction prevents (excitation) light being focused more sharply than $\lambda/(2\mathrm{NA})$, with $\lambda$ being the wavelength of light and NA the numerical aperture of the lens. Thus, as they are illuminated together, features residing any closer together than this distance also fluoresce together and appear in the image as a single blur. The diffraction resolution barrier can be overcome by forcing such nearby features to fluoresce sequentially, but this strategy clearly requires a mechanism for keeping fluorophores that are exposed to excitation light non-fluorescent[1–3].

In stimulated emission depletion (STED) microscopy[1,4], this is accomplished by the so-called STED beam, which turns the fluorescence capability of fluorophores off by a photon-induced de-excitation. Because at least a single de-exciting photon must be available within the lifetime ($\tau \approx 1$–5 ns) of the fluorescent molecular state, the intensity of the focal STED beam must exceed the threshold $I_s = C\tau^{-1}$ with $C$ accounting for the probability of a STED beam photon to interact with the fluorophore[1,4]. The STED beam, usually formed as a doughnut overlaid with the excitation beam, features a central point of zero intensity at which the fluorophores can still assume the fluorescent state. As this point can be positioned with arbitrary precision in space, the coordinate of the emitting (on-state) fluorophores is known at any instant: it is the position of zero intensity[3,5,6] and its immediate vicinity, where the STED beam is still weaker than $I_s$. The diameter of this area is given by $d \approx \lambda/[2\mathrm{NA} \times (1 + I_m/I_s)^{1/2}]$, with $I_m$ (typically $\gg I_s$) denoting the intensity at the doughnut crest. Hence, features that are (just slightly) more apart than $d \ll \lambda/(2\mathrm{NA})$ cannot fluoresce at the same time even when simultaneously illuminated by excitation light[6]. Scanning the beams across the sample and recording the fluorescence yields images of subdiffraction resolution $d$ automatically and irrespective of the fluorophore concentration in the sample.

De-excitation by stimulated emission is the most basic and general mechanism for modulating the fluorescence ability of a molecule. However, by requiring light intensities $> I_s \approx 1$–$10\ \mathrm{MW\ cm^{-2}}$, attaining high resolutions by this mechanism necessitates large $I_m$ values. For example, $d < 40$ nm typically entails $I_m = 100$–$500\ \mathrm{MW\ cm^{-2}}$ (ref. 6). Although intensities of this order have been demonstrated to be live-cell compatible[4,7–10], all-optical nanoscopy methods operating at fundamentally lower light levels are highly in demand[2,5,11–13], because they allow larger fields of view[5,14] and can avoid photodamage.

A route to low light level operation is to replace STED with a fluorescence switching mechanism having a lower threshold $I_s$ (refs 2, 5, 11–13). Following the equation for $I_s$, this can be realized by exploiting transitions between fluorophore states of longer lifetime $\tau \gg 1\ \mu$s (refs 2, 5, 11). Hence, it has been suggested that fluorescence can be switched by transferring the fluorophores transiently to a generic metastable dark (triplet) state of $\tau \approx 10^{-3}$–100 ms (refs 2, 15). A more attractive option is to use fluorophores that can be explicitly 'photoswitched'[5,11], for example, by photoisomerization. Hence, in 2003 it was proposed to implement a STED-like microscope with STED being replaced by a reversible on–off switch as encountered in organic photochromic fluorophores and reversibly photoswitchable fluorescent proteins (RSFPs)[5,11].

In fact, this strategy is even more general because any reversible transition between a signalling and a non-signalling state can be used for breaking the diffraction barrier[15]. Therefore, all concepts that switch the fluorescence capability of molecules at sample coordinates predefined by patterns of light have been generalized under the name RESOLFT[6,12], which stands for reversible saturable optical (fluorescence) transition between two states. Note that a photoswitch is a perfect saturable transition. Concomitantly, the concept was extended to subdiffraction writing[11,13] and data storage, in which case the on-state is a reactive state from which the molecule can be made permanent whereas the off-state serves as a temporary 'mask' defining the structure to be written.

Super-resolution by switching RSFPs was shown in 2005[16], but this study relied on asFP595[17], a tetrameric protein with low fluorescence quantum yield. Moreover, when translating the light pattern across the sample, the proteins faded after a few cycles, implying that features that had been turned off could not be turned on again in order to be

[1]Department of NanoBiophotonics, Max Planck Institute for Biophysical Chemistry, Am Fassberg 11, 37077 Göttingen, Germany. [2]University of Göttingen Medical School, Robert-Koch-Str. 40, 37075 Göttingen, Germany.
*These authors contributed equally to this work.

read out. Biological imaging therefore remained unviable[18]. Other studies using a variant of the RSFP called dronpa[19] faced the same challenge[20]. As a rule of thumb, an *m*-fold resolution improvement along a certain direction requires ~*m* switching cycles, meaning that $m = 10$ along the *x*- and *y*-axes entails ~$m^2 = 100$ cycles, whereas ~1,000 cycles are required for *x*, *y* and *z* (ref. 6). Thus, for RESOLFT super-resolution, the number of switching cycles afforded by the fluorophore assumes a vital role.

Because they are able to generate an image with a single on–off cycle[3,6,21], the super-resolution concepts called (F)PALM[22,23] and STORM[21,24], which have emerged in the interim, have successfully harnessed the switching between metastable states for gaining sub-diffraction resolution. However, these methods rely on the imaging and computation-aided localization of individual fluorophores amidst the scattering and autofluorescence background common in (living) cells and tissues. Moreover, rapid localization of a sufficiently large number of fluorophores requires the excitation light to be intense[22,23]. In contrast, a RESOLFT approach is able to instantly record the emission from all fluorophores attached to the nanosized feature of interest[6], and can be easily combined with confocal microscopy for three-dimensional imaging and background suppression. Yet again, because all RSFPs, conventional fluorescent proteins[25] and photochromic rhodamines[26] seemed unsuitable (Supplementary Fig. 1), an all-optical nanoscopy approach operating at low light levels appeared unviable.

Similarly, although STED/RESOLFT-inspired optical writing with photochromic compounds has been shown to yield structures $<\lambda/(2\mathrm{NA})$, writing such structures with spacings $<\lambda/(2\mathrm{NA})$ remained challenging[27–30], again the impediment being the requirement of many on–off cycles before the structure is made permanent. Here we introduce a RSFP enabling both low-light-level all-optical nanoscopy of living cells and tissues, and far-field optical writing and reading of patterns of subdiffraction size and density.

## Generating a reversibly switchable GFP

All fluorescent proteins have a similar fold, namely an 11-stranded β-barrel with a central helix containing the chromophore, which is typically in a *cis*-configuration[31]. Light-driven switching of RSFPs generally involves an isomerization of the chromophore, frequently coupled with a change of its protonation state[32–36]. We started from EGFP[37] and identified, using its X-ray structure[31], amino acid residues the exchange of which was expected to facilitate isomerization. We expressed numerous EGFP variants in *Escherichia coli* and screened for colonies expressing an RSFP with an automated microscope. To this end, we alternated site-directed and error-prone mutagenesis while maintaining the key amino acids of EGFP (that is, F64L and S65T)[37]; we concomitantly introduced A206K to ensure that the protein remained a monomer[38].

The amino acid exchange Q69L was sufficient to make EGFP(A206K) reversibly switchable, but the resulting on–off contrast was low. Although it makes the protein switchable[39], we avoided the mutation E222Q because it seemed to reduce the number of cycles. After analysing ~30,000 clones, we identified EGFP(Q69L/V150A/V163S/S205N/A206K) (Supplementary Fig. 2) that could be reversibly switched on at $\lambda = 405$ nm and off at 491 nm, and named it reversibly switchable EGFP (rsEGFP).

At equilibrium, rsEGFP adopts a bright on-state (fluorescence quantum yield $\Phi_{FL} = 0.36$; extinction coefficient $\varepsilon = 47{,}000\ \mathrm{M^{-1}\,cm^{-1}}$ (Supplementary Table 1)). In the on-state, rsEGFP exhibits a single absorption band peaking at 491 nm (Fig. 1a), corresponding to the ionized state of the phenolic hydroxyl of the chromophore[40]. The p$K_a$ of the chromophore is 6.5 (Supplementary Fig. 3). Absorption at 490 nm yields fluorescence peaking at 510 nm and, in a competing process, switches rsEGFP off (Figs 1a–c). Prolonged irradiation of a pH 7.5 solution of purified rsEGFP at ~490 nm reduces the rsEGFP fluorescence to 1–2% of its initial value. The off-state exhibits a single absorption band

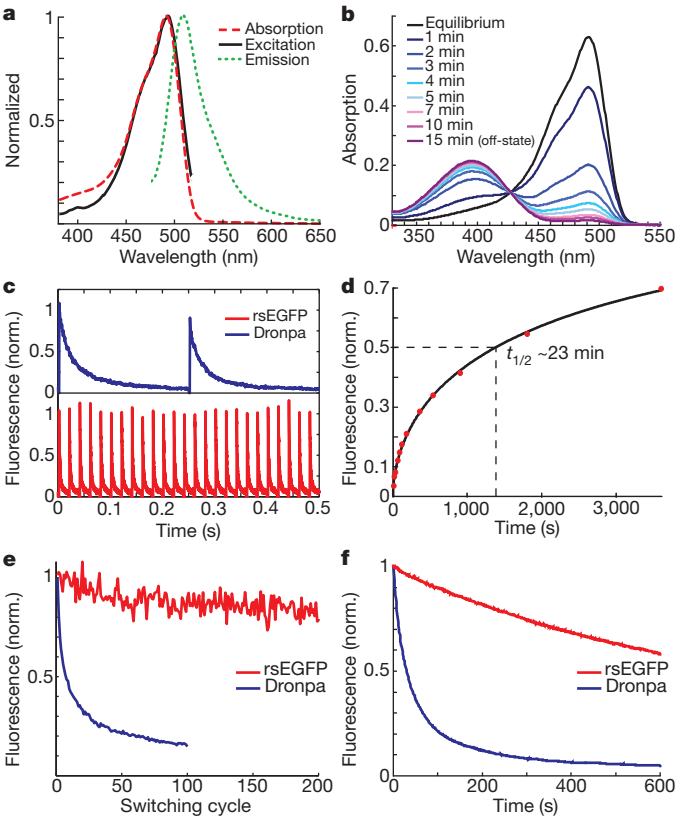


**Figure 1 | Properties of rsEGFP.** **a**, Absorption (red dashed line), excitation (solid black line) and fluorescence (dotted green line) spectrum of rsEGFP in the fluorescent equilibrium state at pH 7.5. **b**, Absorption spectra obtained at different time points during irradiation with 488-nm light. **c**, Switching curves of dronpa (blue) and rsEGFP (red) immobilized in PAA using the same intensities. Switching was performed by alternating irradiation at 405 nm ($2\ \mathrm{kW\,cm^{-2}}$) and at 491 nm ($0.6\ \mathrm{kW\,cm^{-2}}$). The duration of off-switching at 491 nm was chosen such that the fluorescence reached a minimum; irradiation with 405 nm was chosen so that the proteins were fully switched. **d**, Relaxation of rsEGFP embedded in PAA from the off-state into the fluorescent equilibrium state at 22 °C. The black line is a stretched exponential fit with a stretching factor of ~0.6 accounting for inhomogeneous spectral broadening or the involvement of multiple dark states. **e**, Fluorescence per switching cycle normalized to the initial fluorescence, with the same light intensities and switching durations as in **c**. **f**, Photobleaching: rsEGFP and dronpa embedded in a PAA layer were kept in their on-states by continuous irradiation at 405 nm ($1\ \mathrm{kW\,cm^{-2}}$), while fluorescence was probed by irradiation at 491 nm ($3\ \mathrm{kW\,cm^{-2}}$).

at 396 nm, corresponding to the neutral state of the chromophore (Fig. 1b). Excitation at this band switches the protein back to the on-state. At room temperature rsEGFP converts spontaneously from the off- into the on-state with a half-time of ~23 min (Fig. 1d).

We compared the properties of rsEGFP with that of the well-known RSFP dronpa[19]. With the proteins embedded in a 12.5% polyacrylamide (PAA) layer and using light of 491 nm ($0.6\ \mathrm{kW\,cm^{-2}}$) and 405 nm ($2\ \mathrm{kW\,cm^{-2}}$), a complete on–off cycle took 250 ms for dronpa and 20 ms for rsEGFP (Fig. 1c). Dronpa went through <10 cycles before its fluorescence was reduced to 50%, whereas rsEGFP went through ~1,200 cycles under the same conditions (Fig. 1e). To compare bleaching, dronpa and rsEGFP were kept in the on-state by continuous irradiation at 405 nm ($1\ \mathrm{kW\,cm^{-2}}$) while fluorescence was generated by irradiation at 491 nm ($3\ \mathrm{kW\,cm^{-2}}$). Whereas dronpa fluorescence was reduced to 50% within $t_{1/2} \approx 30$ s, for rsEGFP we measured $t_{1/2} \approx 800$ s (Fig. 1f). The rsEGFP chromophore maturated with a half-time of ~3 h at 37 °C (Supplementary Fig. 4). The protein behaved as a monomer *in vitro* (Supplementary Fig. 5), could be fused to various proteins, including α-tubulin and histone H2B (Supplementary Fig. 6), and was repeatedly switchable in living cells (Supplementary Fig. 7).

## Rewritable data storage

To analyse whether immobilized rsEGFP could be used for repeated short-term data storage[41], we coated a microscope slide with a <1-μm thin layer of rsEGFP (~0.03 mM) in PAA. Switching and reading by illumination at 405 nm and 491 nm in a scanning confocal set-up provided an on–off contrast of ~50:1. We translated the text of 25 Grimm's fairy stories (http://www.gutenberg.org/files/11027/11027.txt) into 7-bit binary ASCII code ('0': off; '1': on) and wrote and read the ~270,000 letters into a 17 μm × 17 μm region in 6,596 frames, each comprising 41 letters (287 bits) (Fig. 2). Individual bits were ~0.5 μm in diameter with 1 μm centre-to-centre spacing, corresponding to a DVD storage density. Discriminating '0' from '1' by a simple threshold entailed 7 bit errors within the entire data set. After ~6,600 read/write cycles in the same region, the average fluorescence of the '1' was reduced by ~35% (Supplementary Fig. 8). Hence, the same rsEGFP layer can be used for ~15,000 read/write processes.

## RESOLFT nanoscopy of living samples

Next, we implemented a scanning confocal set-up with a 405 nm (ultraviolet) beam for switching the rsEGFP on, a 491 nm (blue) beam for eliciting fluorescence, and a doughnut-shaped 491 nm beam for the off-switching (Supplementary Fig. 9). We fused rsEGFP to the amino-terminus of the bacterial actin homologue MreB[42] and expressed the fusion protein in *E. coli* bacteria. Living bacteria on agar-coated slides were recorded by first irradiating each pixel for 100 μs with ultraviolet light (1 kW cm$^{-2}$), thus activating most of the rsEGFP in the focal volume. Then the doughnut-shaped blue beam ($I_m \approx 1$ kW cm$^{-2}$) was applied for 10–20 ms to switch all the rsEGFP molecules off, except those located within $d/2$ distance from the doughnut centre. Lastly, the rsEGFP fluorescence was read out for 1–2 ms by the 491-nm beam (~1 kW cm$^{-2}$). The sequence was repeated for each sample pixel.

The double-helical cytoskeletal structure of rsEGFP–MreB is more clearly revealed by RESOLFT than by its confocal counterpart (Fig. 3a). The RESOLFT image of a typical filament showed a full-width half-maximum (FWHM) of ~70 nm. Because this value seemed to be determined by the thickness of the filament itself, a more accurate upper limit for the resolution $d$ is obtained by imaging the finer keratin-19–rsEGFP intermediate filament network in living mammalian cells (Fig. 3b, c). Line profiles from recorded data gave $d < 40$ nm corresponding to a 5–6-fold all-optical resolution improvement over confocal microscopy (Fig. 3c).

To investigate its applicability to living brain tissue, we locally injected viral particles carrying a lifeact–rsEGFP construct into a cultured organotypical hippocampal brain slice. Lifeact is a 17-amino-acid-long peptide with high affinity to filamentous actin[43]. RESOLFT revealed fine morphological differences between the spines protruding from a dendrite (Fig. 3d). A profile through a spine neck showed a FWHM of <80 nm. Electron microscopy of similar samples demonstrated that this value is close to the actual size of the spine necks themselves[44], suggesting a resolution $d$ substantially <80 nm. Repeated imaging revealed dynamic changes over 5 min (Fig. 3d). Altogether, the resolution is comparable to that provided by STED

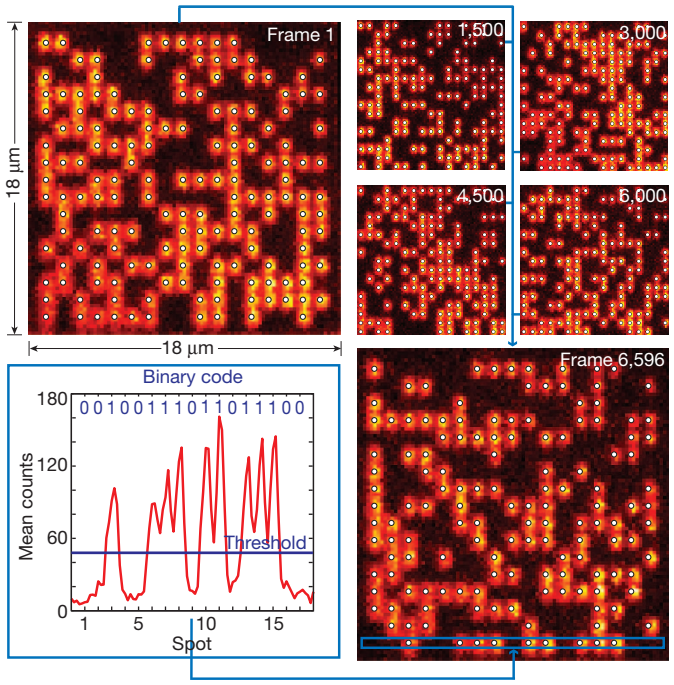


**Figure 2 | Rewritable data storage.** The text of 25 Grimm's fairy stories (ASCII code; 1.9 Mbits) consecutively written and read on a 17 × 17 μm area of a PAA layer containing rsEGFP, with bits written as spots (representative frames shown). The white dots mark spots that were recognized as set bits ('1's). The graph shows an intensity profile along the indicated area, averaged over three pixels along the *y*-axis. The blue line indicates the threshold used to assign read spots to '0's or '1's.

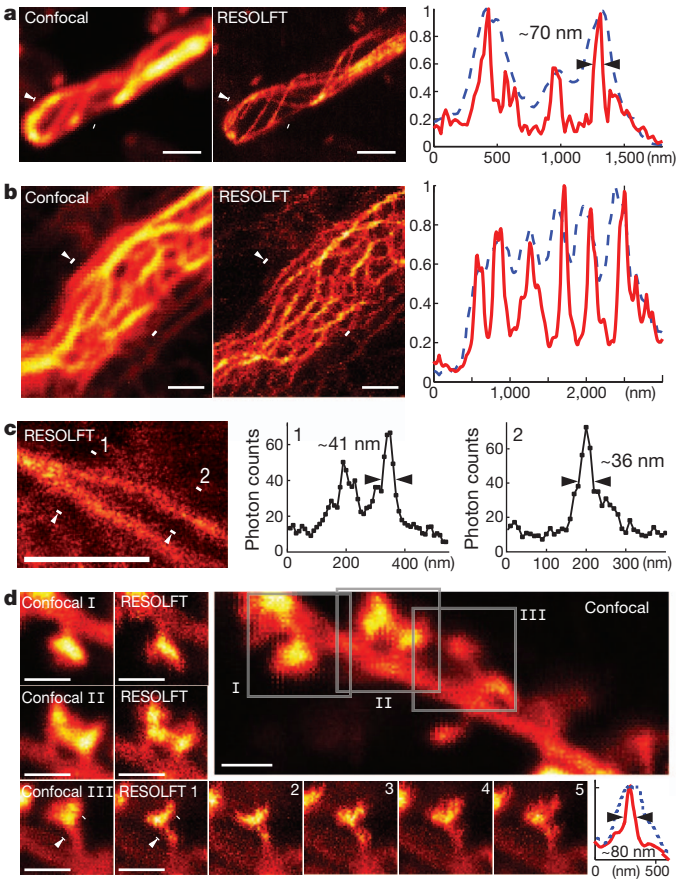


**Figure 3 | RESOLFT nanoscopy of living cells.** **a**, *E. coli* bacterium expressing rsEGFP–MreB: confocal (left) and corresponding RESOLFT (middle) image. **b**, Mammalian (PtK2) cell expressing keratin-19–rsEGFP imaged in the confocal (left) and the RESOLFT (middle) mode. **a**, **b**, Graphs show the normalized fluorescence profiles between the two white markers with the white arrowhead indicating the direction (solid red, RESOLFT; dashed blue, confocal). **c**, RESOLFT image (left) of keratin-19–rsEGFP filaments in a PtK2 cell recorded with a pixel size of 10 nm × 10 nm; smoothed with a low-pass Gaussian filter of 1.2 pixel width. Graphs 1 and 2 extracted from the image as indicated reveal resolution $d < 40$ nm. **d**, Dendrite within a living organotypic hippocampal slice expressing lifeact–rsEGFP. Main image: confocal overview. I–III: three spines, as indicated on the main image, each imaged in the confocal (left) and the RESOLFT mode (right). Spine III was repeatedly imaged in the RESOLFT mode within 5 min, demonstrating the changes over time. Graph: normalized profile across a spine neck as imaged in the RESOLFT (solid red) or the confocal mode (dashed blue) between the two white markers. Scale bars, 1 μm.

on similar structures[10], but here it is obtained with light intensities lower by about a million times.

## RESOLFT optical data storage

For investigating subdiffraction resolution writing, an rsEGFP layer was prepared as previously outlined. The writing entailed (1) an ultraviolet beam (405 nm, 1 kW cm$^{-2}$) applied for 100 µs to switch rsEGFP on, (2) a 2-ms break for equilibration, (3) a doughnut-shaped blue beam (491 nm, 0.5 kW cm$^{-2}$) lasting 20 ms confining the on-state within $d/2$ around the doughnut centre, and (4) an ~2-ms 532 nm beam (~900 kW cm$^{-2}$) for transferring on-state rsEGFP to a permanent off (bleached) state (Fig. 4a) (Supplementary Fig. 10a). Lastly, the rsEGFP molecules located outside this region were switched back on, which is critical for writing another feature within subdiffraction proximity.

We wrote nine patterns of 3 × 3 bit fields in an rsEGFP layer, with 250 nm centre-to-centre separation between individual bits (Fig. 4b), both in the conventional and in the RESOLFT mode. Whereas conventional writing and/or confocal reading blurred the data, the bits were fully discernible when both writing and reading were performed by RESOLFT. We wrote and read the data down to distances of 200 nm between the individual bits (Supplementary Fig. 10b). Hence this scheme allowed storing and reading out bits ~4 times more densely than by regular focusing. The structures could be read 5–10 times.

## Discussion and conclusion

The many-switching cycles afforded by the fluorescence protein rsEGFP reported here has facilitated live-cell RESOLFT microscopy, a super-resolution microscopy that is similar to STED microscopy in usability but operates at ~$10^6$ times lower levels of light. Multiphoton-induced optical damage[45] can therefore be virtually excluded. The fundamental reduction in optical intensity required for the on–off switching stems from the fact that the fluorescence capability of the molecule is not modulated by disallowing the population of its nanosecond fluorescent state, but rather by toggling it between two long-lived ground states, one in which the fluorophore remains dark when exposed to the excitation light.

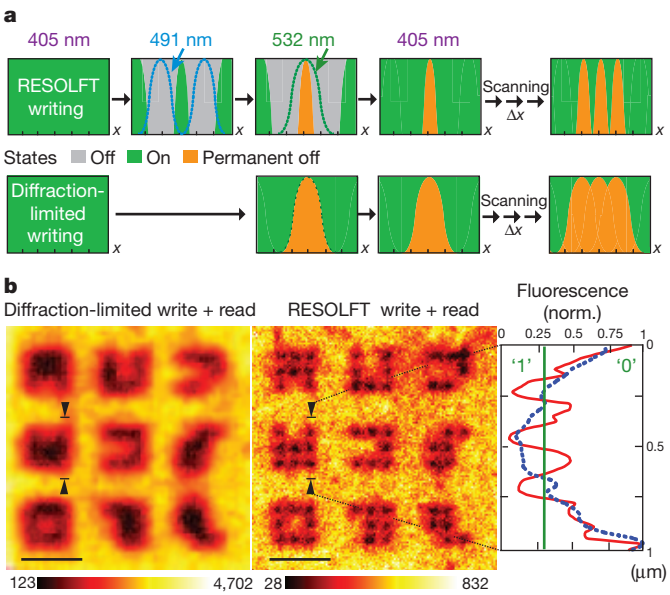


**Figure 4 | Subdiffraction-resolution writing and reading using rsEGFP and visible light.** **a**, Top, schematic of RESOLFT writing: rsEGFP molecules are switched off at 491 nm using a doughnut-shaped focal intensity (dashed blue line) so that the on-state is confined to a subdiffraction-sized region around the doughnut centre. Subsequent irradiation with 532-nm light makes the on-state molecules permanent by bleaching. Irradiation at 405 nm switches the off-state molecules back into the on-state, allowing the writing of another feature in subdiffraction proximity. Bottom, schematic of diffraction-limited writing. **b**, Conventional (left) and subdiffraction RESOLFT (middle) joined writing and reading in a layer of immobilized rsEGFP. The outlines of the corresponding 3 × 3 bit patterns were identical. The distance between two bleached spots was 250 nm in each case. Right, normalized line profiles of the fluorescence signal between the two arrows (solid red, RESOLFT; dashed blue, confocal). Scale bars, 1 µm.

RESOLFT is readily combined with confocal imaging, which increases its use in scattering living samples. In fact, the imaging of neuronal spines in living organotypical brain slices testifies this potential. Although the recording time reported here is still of the order of most other super-resolution techniques[3,6,21] and slower than the fastest biological STED recordings[7], by gathering the signal from typically many molecules located at predefined positions, RESOLFT has all the prerequisites for fast imaging. Scanning with arrays of doughnuts or zero-intensity lines (so-called structured illumination[5,14,18,46]) and detection by a camera will reduce the number of scanning steps required to cover large fields of view and facilitate low-intensity video-rate imaging. The maximum recording speed is determined by the time it takes to establish the disparity of (on–off) states in space, that is, by the switching kinetics, which probably can be improved by further mutagenesis. Note that the switching is not restricted to changes in brightness (on–off) only. Other reversible transitions between disparate states may also prove suitable for RESOLFT imaging, such as states yielding differences in emission wavelengths, lifetime or polarization.

Photoswitching between long-lived states also poses challenges, because in the process the molecule can assume transient (dark) states, such as triplet states, which depend on the molecular microenvironment. In this regard, STED maintains a unique advantage because it entails just basic optical transitions between the ground and the fluorescent state; no atom relocation, spin flip or change in chemical bond is required to switch the fluorescence capability of the molecule — just light. Therefore, switching fluorescence by STED is nearly universal and instantaneous.

The switching stamina of rsEGFP also enabled writing and reading of patterns of both subdiffraction size and spacing $d$, which has so far been difficult for direct far-field optical writing. In our study, the smallest obtainable structure size was co-determined by the fact that the 532-nm light moderately bleached the off-state proteins too, thus reducing the writing contrast. However, this initial demonstration should spur on new advancements in this field, because current nanowriting efforts are dominated by concepts that resort to much shorter wavelengths of electromagnetic radiation at which focusing becomes exceedingly difficult. In fact, RESOLFT and related concepts are unique for creating materials that are nanostructured in three dimensions[30]. To maximize the resolution along the optical axis ($z$), RESOLFT imaging and writing can also be combined with 4Pi microscopy[47], in which case three-dimensional resolution of <10 nm should become possible at ultralow light levels.

The resolution demonstrated here is similar or even exceeds the resolution attained until now by STED in living cells[8,10]. Although in both methods the resolution can be continually increased by increasing $I_m/I_s$, in STED microscopy this strategy will reach practical limits due to the intensities required. Using a threshold intensity $I_s$ that is lower by many orders of magnitude, switching between long-lived states overcomes these limits and, as we have demonstrated here, offers a pathway to lens-based optical imaging and writing at molecular dimensions.

## METHODS SUMMARY

**Protein generation and screening.** Site-directed mutagenesis was performed with the QuikChange Site Directed Mutagenesis Kit (Stratagene) or a multiple-site approach using several degenerative primers. The proteins were expressed from the high-copy expression vector pQE31 (Qiagen) and expressed in *E. coli*.

**Viral transfection.** A modified Semliki Forest Virus containing the pSCA-Lifeact-rsEGFP vector construct was injected into the slice cultures using a patch pipette. Imaging was performed within 16–48 h after incubation.

**Data storage.** A layer containing immobilized rsEGFP was prepared by mixing 24.5 µl purified proteins (0.09 mM) with 17.5 µl Tris-HCl pH 7.5, 30 µl acrylamide (Rotiphorese Gel 30, Roth), 0.75 µl 10% ammonium persulfate and 1 µl 10%

TEMED. About 10 µl of this solution was placed on a glass slide and a cover slip was pressed onto the sample to attain a thin layer. Custom MATLAB (The MathWorks) programs allowed automated generation of the voltages and signals for moving the sample and for generating the desired laser pulses. Images were also taken using the software Imspector (http://www.imspector.de).

**RESOLFT set-up.** We implemented a home-built confocal microscope with a normally focused beam for generating fluorescence plus a doughnut-shaped beam for switching rsEGFP off (both at 491 nm wavelength). The beams were circularly polarized, superimposed in the focal plane and applied sequentially. The 405 nm beam for switching rsEGFP on was also circularly polarized. The fluorescence emitted between 500–560 nm was imaged on the opening of a multi-mode fibre and detected by a counting avalanche photodiode. The same set-up was used for writing, which was most specific at 532 nm.

Full details of methods used are available in Supplementary Information.

**Received 23 May; accepted 24 August 2011.**
**Published online 11 September 2011.**

1. Hell, S. W. & Wichmann, J. Breaking the diffraction resolution limit by stimulated emission: stimulated-emission-depletion fluorescence microscopy. *Opt. Lett.* **19,** 780–782 (1994).
2. Hell, S. W. & Kroug, M. Ground-state depletion fluorescence microscopy, a concept for breaking the diffraction resolution limit. *Appl. Phys. B* **60,** 495–497 (1995).
3. Hell, S. W. Far-field optical nanoscopy. *Science* **316,** 1153–1158 (2007).
4. Klar, T. A., Jakobs, S., Dyba, M., Egner, A. & Hell, S. W. Fluorescence microscopy with diffraction resolution barrier broken by stimulated emission. *Proc. Natl Acad. Sci. USA* **97,** 8206–8210 (2000).
5. Hell, S. W. Toward fluorescence nanoscopy. *Nature Biotechnol.* **21,** 1347–1355 (2003).
6. Hell, S. W. Microscopy and its focal switch. *Nature Methods* **6,** 24–32 (2009).
7. Westphal, V. *et al.* Video-rate far-field optical nanoscopy dissects synaptic vesicle movement. *Science* **320,** 246–249 (2008).
8. Hein, B., Willig, K. I. & Hell, S. W. Stimulated emission depletion (STED) nanoscopy of a fluorescent protein-labeled organelle inside a living cell. *Proc. Natl Acad. Sci. USA* **105,** 14271–14276 (2008).
9. Eggeling, C. *et al.* Direct observation of the nanoscale dynamics of membrane lipids in a living cell. *Nature* **457,** 1159–1162 (2009).
10. Nägerl, U. V., Willig, K. I., Hein, B., Hell, S. W. & Bonhoeffer, T. Live-cell imaging of dendritic spines by STED microscopy. *Proc. Natl Acad. Sci. USA* **105,** 18982–18987 (2008).
11. Hell, S. W., Jakobs, S. & Kastrup, L. Imaging and writing at the nanoscale with focused visible light through saturable optical transitions. *Appl. Phys., A Mater. Sci. Process.* **77,** 859–860 (2003).
12. Hell, S. W., Dyba, M. & Jakobs, S. Concepts for nanoscale resolution in fluorescence microscopy. *Curr. Opin. Neurobiol.* **14,** 599–609 (2004).
13. Hell, S. W. Strategy for far-field optical imaging and writing without diffraction limit. *Phys. Lett.* **326,** 140–145 (2004).
14. Gustafsson, M. G. L. Nonlinear structured-illumination microscopy: wide-field fluorescence imaging with theoretically unlimited resolution. *Proc. Natl Acad. Sci. USA* **102,** 13081–13086 (2005).
15. Hell, S. W. in *Topics in Fluorescence Spectroscopy* Vol. 5 (ed. Lakowicz, J. R.) 361–422 (Plenum, 1997).
16. Hofmann, M., Eggeling, C., Jakobs, S. & Hell, S. W. Breaking the diffraction barrier in fluorescence microscopy at low light intensities by using reversibly photoswitchable proteins. *Proc. Natl Acad. Sci. USA* **102,** 17565–17569 (2005).
17. Lukyanov, K. A. *et al.* Natural animal coloration can be determined by a nonfluorescent green fluorescent protein homolog. *J. Biol. Chem.* **275,** 25879–25882 (2000).
18. Schwentker, M. A. *et al.* Wide-field subdiffraction RESOLFT microscopy using fluorescent protein photoswitching. *Microsc. Res. Tech.* **70,** 269–280 (2007).
19. Ando, R., Mizuno, H. & Miyawaki, A. Regulated fast nucleocytoplasmic shuttling observed by reversible protein highlighting. *Science* **306,** 1370–1373 (2004).
20. Dedecker, P. *et al.* Subdiffraction imaging through the selective donut-mode depletion of thermally stable photoswitchable fluorophores: numerical analysis and application to the fluorescent protein dronpa. *J. Am. Chem. Soc.* **129,** 16132–16141 (2007).
21. Huang, B., Babcock, H. & Zhuang, X. Breaking the diffraction barrier: super-resolution imaging of cells. *Cell* **143,** 1047–1058 (2010).
22. Betzig, E. *et al.* Imaging intracellular fluorescent proteins at nanometer resolution. *Science* **313,** 1642–1645 (2006).
23. Hess, S. T., Girirajan, T. P. K. & Mason, M. D. Ultra-high resolution imaging by fluorescence photoactivation localization microscopy. *Biophys. J.* **91,** 4258–4272 (2006).
24. Rust, M. J., Bates, M. & Zhuang, X. Sub-diffraction-limit imaging by stochastic optical reconstruction microscopy (STORM). *Nature Methods* **3,** 793–796 (2006).
25. Dickson, R. M., Cubitt, A. B., Tsien, R. Y. & Moerner, W. E. On/off blinking and switching behaviour of single molecules of green fluorescent protein. *Nature* **388,** 355–358 (1997).
26. Bossi, M., Foelling, J., Dyba, M., Westphal, V. & Hell, S. W. Breaking the diffraction resolution barrier in far-field microscopy by molecular optical bistability. *N. J. Phys.* **8,** 275 (2006).
27. Scott, T. F., Kowalski, B. A., Sullivan, A. C., Bowman, C. N. & McLeod, R. R. Two-color single-photon photoinitiation and photoinhibition for subdiffraction photolithography. *Science* **324,** 913–917 (2009).
28. Li, L., Gattass, R. R., Gershgoren, E., Hwang, H. & Fourkas, J. T. Achieving l/20 resolution by one-color initiation and deactivation of polymerization. *Science* **324,** 910–913 (2009).
29. Andrew, T. L., Tsai, H. Y. & Menon, R. Confining light to deep subwavelength dimensions to enable optical nanopatterning. *Science* **324,** 917–921 (2009).
30. Fischer, J., Freymann, G. & Wegener, M. The materials challenge in diffraction-unlimited direct-laser-writing optical lithography. *Adv. Mater.* **22,** 3578–3582 (2010).
31. Ormö, M. *et al.* Crystal structure of the *Aequorea victoria* green fluorescent protein. *Science* **273,** 1392–1395 (1996).
32. Andresen, M. *et al.* Structure and mechanism of the reversible photoswitch of a fluorescent protein. *Proc. Natl Acad. Sci. USA* **102,** 13070–13074 (2005).
33. Andresen, M. *et al.* Structural basis for reversible photoswitching in Dronpa. *Proc. Natl Acad. Sci. USA* **104,** 13005–13009 (2007).
34. Henderson, J. N., Ai, H. W., Campbell, R. E. & Remington, S. J. Structural basis for reversible photobleaching of a green fluorescent protein homologue. *Proc. Natl Acad. Sci. USA* **104,** 6672–6677 (2007).
35. Adam, V. *et al.* Structural characterization of IrisFP, an optical highlighter undergoing multiple photo-induced transformations. *Proc. Natl Acad. Sci. USA* **105,** 18343–18348 (2008).
36. Brakemann, T. *et al.* Molecular basis of the light-driven switching of the photochromic fluorescent protein Padron. *J. Biol. Chem.* **285,** 14603–14609 (2010).
37. Patterson, G. H., Knobel, S. M., Sharif, W. D., Kain, S. R. & Piston, D. W. Use of the green fluorescent protein and its mutants in quantitative fluorescence microscopy. *Biophys. J.* **73,** 2782–2790 (1997).
38. Zacharias, D. A., Violin, J. D., Newton, A. C. & Tsien, R. Y. Partitioning of lipid-modified monomeric GFPs into membrane microdomains of live cells. *Science* **296,** 913–916 (2002).
39. Bizzarri, R. *et al.* Single amino acid replacement makes *Aequorea victoria* fluorescent proteins reversibly photoswitchable. *J. Am. Chem. Soc.* **132,** 85–95 (2010).
40. Tsien, R. Y. The green fluorescent protein. *Annu. Rev. Biochem.* **67,** 509–544 (1998).
41. Adam, V. *et al.* Data storage based on photochromic and photoconvertible fluorescent proteins. *J. Biotechnol.* **149,** 289–298 (2010).
42. Vats, P. & Rothfield, L. Duplication and segregation of the actin (MreB) cytoskeleton during the prokaryotic cell cycle. *Proc. Natl Acad. Sci. USA* **104,** 17795–17800 (2007).
43. Riedl, J. *et al.* Lifeact: a versatile marker to visualize F-actin. *Nature Methods* **5,** 605–607 (2008).
44. Harris, K. M. & Kater, S. B. Dendritic spines: cellular specializations imparting both stability and flexibility to synaptic function. *Annu. Rev. Neurosci.* **17,** 341–371 (1994).
45. Hopt, A. & Neher, E. Highly nonlinear photodamage in two-photon fluorescence microscopy. *Biophys. J.* **80,** 2029–2036 (2001).
46. Heintzmann, R., Jovin, T. M. & Cremer, C. Saturated patterned excitation microscopy—a concept for optical resolution improvement. *JOSA A* **19,** 1599–1609 (2002).
47. Hell, S. W., Schmidt, R. & Egner, A. Diffraction-unlimited three-dimensional optical nanoscopy with opposing lenses. *Nature Photon.* **3,** 381–387 (2009).

**Supplementary Information** is linked to the online version of the paper at www.nature.com/nature.

**Acknowledgements** We thank J. Jethwa for careful reading and M. Andresen, T. Brakemann, S. Löbermann, R. Schmitz-Salue and A. C. Stiel for discussions and support, as well as T. Gilat and F. Voss (MPI of Neurobiology, Munich) for help with the slice culture preparation and A. Schönle for adapting the software Imspector. We thank The Project Gutenberg for making Grimm's Fairy Tales available in electronic format, L. Rothfield (University of Connecticut Health Center) for providing the plasmid pLE7, R. Wedlich-Söldner (MPI of Biochemistry, Munich) for the lifeact–YFP construct and V. Stein (MPI of Neurobiology, Munich) for the virus protocol. This work was supported by the Deutsche Forschungsgemeinschaft (DFG) through the DFG-Research Center for Molecular Physiology of the Brain (to S.J.) and by a Gottfried-Wilhelm-Leibniz prize of the DFG (to S.W.H.).

**Author Contributions** T.G., I.T., M.L., H.B., F.L.-C. performed research, I.T., M.L., T.G., H.B., C.E. set up the microscopes, N.T.U., K.I.W. prepared samples, M.L., T.G., I.T., K.I.W., S.J., S.W.H. analysed data, S.J., C.E., S.W.H. designed research. S.J., M.L., S.W.H. wrote the paper. All authors discussed the data and commented on the manuscript.

**Author Information** Reprints and permissions information is available at www.nature.com/reprints. The authors declare no competing financial interests. Readers are welcome to comment on the online version of this article at www.nature.com/nature. Correspondence and requests for materials should be addressed to S.J. (sjakobs@gwdg.de) or S.W.H. (shell@gwdg.de).